Chemical Physics Letters, Volume 715, January 2019, pp. 181-185
DOI:10.1016/j.cplett.2018.11.041

Mechanical Impregnation of Pd-Sn/alumina and Cu-Mn/graphite on Charcoal to Minimise Carbon monoxide Emissions

Nyombi A[a,*] , Williams M. R[b], Wessling R[a]

[a]*Cranfield Forensic Institute – Cranfield University – Defence Academy of the United Kingdom - Shrivenham. SN6 8LA*

[b]*Center for Defence Chemistry - Cranfield University – Defence Academy of the United Kingdom - Shrivenham. SN6 8LA*

Abstract

This study investigated how to minimize carbon monoxide (CO) emissions from charcoal by impregnating with Pd-Sn/alumina and Cu-Mn/graphite. Samples were heated isothermally with continuous monitoring of residual CO using electrochemical and infra-red sensors. With 0.2wt% Pd-Sn/alumina, 26.9% and 44.4% were recorded as lowest and highest residual CO. On the other hand, when 2wt% Cu-Mn/graphite was used, 15.6%, and 25.3% were observed as lowest and highest residual CO. The activity of the catalysts decreased with temperature and increased with catalyst loading. This method could be used on briquettes, wood boiler chips and other solid carbonaceous materials to minimise CO emissions.

Keywords: Carbon monoxide; catalyst-impregnated charcoal; residual CO

Declarations of interest: none

* Corresponding Author – Nyombi Antony
E-mail – a.nyombi@cranfield.ac.uk
Cranfield University – Shrivenham, SN6 8LA

Graphical Abstract

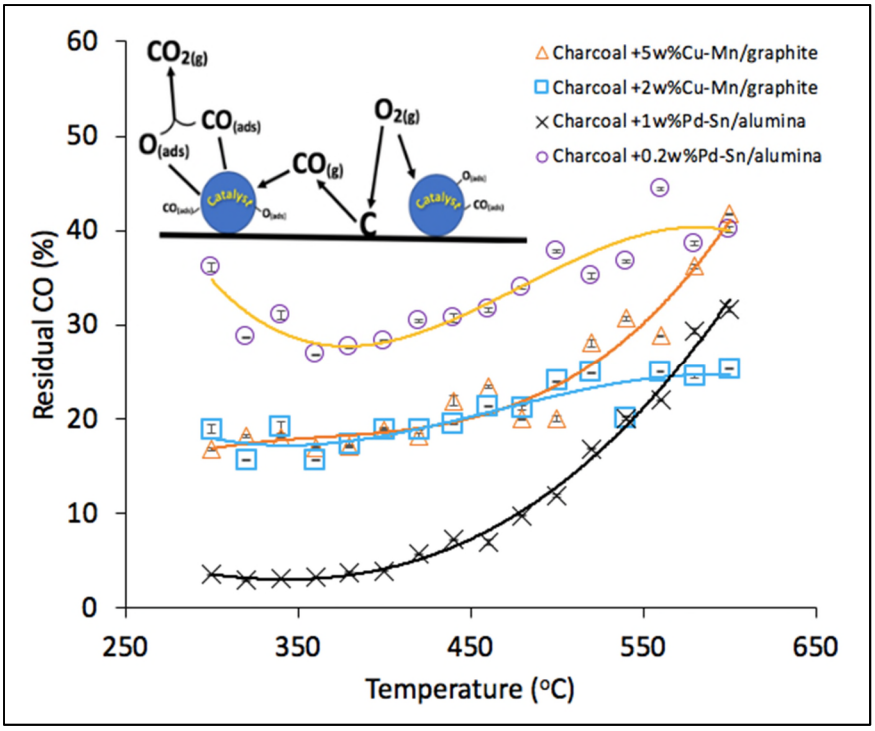

1 Introduction

Charcoal from woody biomass is one of the high energy materials (calorific value ≈ 30MJ/kg) used for cooking and heating. As it burns, charcoal releases several by-products that are dependent on its properties and the prevailing conditions. Complete combustion yields mainly carbon dioxide (CO_2) and moisture while incomplete combustion yields carbon monoxide (CO), carbon dioxide, particulate matter, volatile organic compounds, carbonyls among others [1]. Charcoal usage has led to a lot of unintentional CO poisoning resulting in the death of many people with countless near misses and chronic injuries [2], [3], [4], [5]. On the other hand, CO poisoning from charcoal has been used as a method to commit suicide [6], [7], [8], [9].

Efforts have been made through combustion equipment design to achieve near-complete combustion [10], [11], [12], [13], [14] for maximum CO oxidation. However, these systems have not been very successful, and they still expose charcoal users to high concentrations of CO. Other researchers have resorted to CO oxidation using metal/metal oxide catalysts or several combinations.

The unique adsorption properties and reactivity of CO on metal/oxide surfaces have enabled researchers to oxidize it to CO_2. The chemisorption behavior of CO on metals has been reported to vary considerably, with the heats of chemisorption increasing with the metal surface density for platinum, rhodium, and ruthenium. For palladium and iridium, a reverse order was observed; heats of chemisorption followed the trend - Pd≈Ir>Pt>Rh>Ru≈Ni>Co>> Cu. There is a general decrease in heats of chemisorption on metal surfaces with CO and O_2 coverage. Oxygen is chemisorbed dissociatively on metal surfaces, with the heats of dissociative chemisorption decreasing in the order: W>Mo>Fe>Co>Ir≈Ru>Rh≈Ni>Cu>Pt>Pd>Ag> Au [15].

The presence of a supporting material has a crucial effect on the activity of metal/ oxide catalysts. For example, CuO is unstable when not supported, and the oxidation state of copper usually varies depending on temperature and the CO:O_2 ratio. The three oxidation states (Cu^{2+}, Cu^{+} and even Cu^{0}) may coexist, during a reaction. Addition of a support like zirconia or alumina to CuO increases its activity by 10 to 200-fold. Supported copper oxide catalysts are also more tolerant to potential poisons like SO_2. The support enhances the co-existence of Cu^{2+}, Cu^{+}, and Cu^{0} species especially when appropriate pre-treatments are applied or by using the right set of supports. However, the catalyst is deactivated by moisture [15]. Manganese/oxides work best with other elements, like copper, cobalt, Nickel, and Lanthanum, forming manganites. This combination enhances Mn as a catalyst for oxidation of CO. It forms three principal oxides: MnO_2, Mn_2O_3 or Mn_3O_4. Mn_2O_3 is the most stable and very active. It has four polymorphs, denoted as alpha-, beta-, gamma-, and delta-MnO_2. Alpha- and delta-MnO_2 are the most active polymorphs for CO oxidation compared to gamma- and beta-MnO_2. This is attributed to the strength of the Mn-O bond (alpha<delta<gamma<beta); with the strongest Mn-O bond responsible to less activity of the corresponding oxide [15].

Fuchs *et al*. [16] found that the rate of adsorption of CO was controlled by the oxidation of CO using palladium. The adsorption on the metal surface follows the Langmuir-Hinshelwood mechanism [17], [18]. Bi *et al*. [19] found that the CO oxidation activity of Pd/NaZSM-5 decreased with the increase of calcination temperature and increased with the increase of Pd concentration. The decreased activity with calcination could be linked to the increase in crystallinity of the support and decrease in metal/support interaction [20].

Kondrat *et al*. [21] found that the ability to control phase formation (Cu-oxides and Mn-oxides) in Cu-Mn/support catalyst with heat treatment allows their catalytic potential for CO oxidation to be assessed. The presence of the $CuMn_2O_4$ phase within the catalyst mix is linked to high activity for CO oxidation. Retention of carbon dioxide as a by-product as well as contact with moisture poisons the catalyst, however, expelling the moisture at moderate temperatures restores the catalytic activity [22]. The activity of Cu-Mn generally decreases with temperature [23]. Highly homogeneous catalysts are found to be more active than less homogeneous ones for ambient temperature oxidation of CO [24].

All the studies mentioned above have done CO oxidation by passing the gas through/over a catalyst either in a fixed bed or a reactor of some sort. Up-to-date, there has not been any study focusing on ensuring the safety of charcoal by impregnating it with catalysts. This study differentiates itself by mechanically mixing the catalysts with charcoal to form a product with high homogeneity. Commercial Pd-Sn/alumina and Cu-Mn/graphite have been used in this study. Different concentrations of the catalysts were mixed with the charcoal mechanically, and the catalyst activity was tested by heating the product isothermally at different temperatures in the range 300-600^{o}C with residual CO measurement and recording. The catalyst activity was tested by monitoring the residual CO evolved as a function of temperature and catalyst concentration.

2 Methodology

2.1 Materials

Charcoal used in this study was produced using a controlled laboratory muffle furnace by pyrolysis of wood in a sealed retort heated for 4 hours at 500^{o}C. This charcoal was ground by a laboratory vibratory pulverizer (Essa LM2 pulverizing mill) and sieved through a 210μm mesh. Commercial catalysts, Pd-Sn/alumina) and Cu-Mn/graphite purchased from Moleculite Products Limited were mechanically mixed together with the charcoal in different proportions (0.2w%, 1w%, 2w%, 5w% - catalyst) in a mortar and pestle to achieve a homogeneous product.

2.2 Material characterisation

The commercial catalysts Pd-Sn/alumina and Cu-Mn/graphite as well as the catalyst treated charcoal were characterised using thermogravimetric analysis (TGA), X-Ray Diffraction

(XRD), and X-Ray Fluorescence (XRF). Thermogravimetric analysis was performed on a Mettler Toledo DSC/TGA3+ in an air environment at 50ml/min, with a non-isothermal mode. Diffraction patterns were recorded with a Panalytical X'Pert diffractometer using Cu-Kα radiation. The powdered catalyst was loaded on to low background scattering (off-cut silicon) XRD holders. A PIXcel strip detector was used to collect data as stepped scans across an angular range of 10 to 80 2θ degrees. The quantities of elements present in the ash were analysed using the SEA6000VX bench-top X-ray fluorescence instrument manufactured by Seiko instruments (Nano technology Incorporated). The measurement conditions used were; a sample standard (RTC-CRM002-100G from LGC) and a Rhodium tube as the target. The analysis conditions were; measurement time (100 seconds), collimator/spot size (1.2X1.2mm), tube voltage (50kV), tube current (314μA - in Auto mode), no filter and He purging environment

2.3 Testing catalyst activity

Approximately 200mg of the catalyst impregnated charcoal was tested for residual CO evolution. Charcoal samples were weighed (on an HF-300G analytical balance with an accuracy of ±0.002g) into a quartz boat and loaded into a quartz tube (diameter = 35 mm, length = 550 mm) in a horizontal Carbolite tube furnace, which had been pre-heated to a set temperature with a regulated constant air flow. The experiments were conducted isothermally, and the temperature of the furnace was controlled using a Eurotherm CTFI-1200 controller. Samples were heated at 300, 320,340, 360, 380, 400, 420, 440, 460, 480,500, 520, 540, 560, 580, and 600°C, (with a combined uncertainty of ±5°C) and at an air flow rate of 2± 0.1 (L/min) (all values are ± combined uncertainty). Air flow was controlled by a calibrated ($R^2 = 0.99$) Platon rotameter flow meter. The CO was channelled through a 0.8-μm cellulose membrane filter, to remove any smoke particles, to a CO sensor which gave an output to a Squirrel 1200 data logger and recorded voltages at a rate of four data points per minute **Fig. 1**. The logger display was regularly inspected during the heating period until the reading had fallen to zero CO (indicating emissions were below the detection limit for the sensor). The sensor was calibrated by injecting measured volumes of pure CO from a gas-tight syringe into several Tedlar bags which had been filled with air from a cylinder at a known flow rate for a known length of time. Calibration graphs were constructed to cover the range of concentrations that the sensors could measure. The calibration graph ($R^2 = 0.99$) was

used to calculate the concentrations of CO. All CO measurement experiments were performed in triplicate.

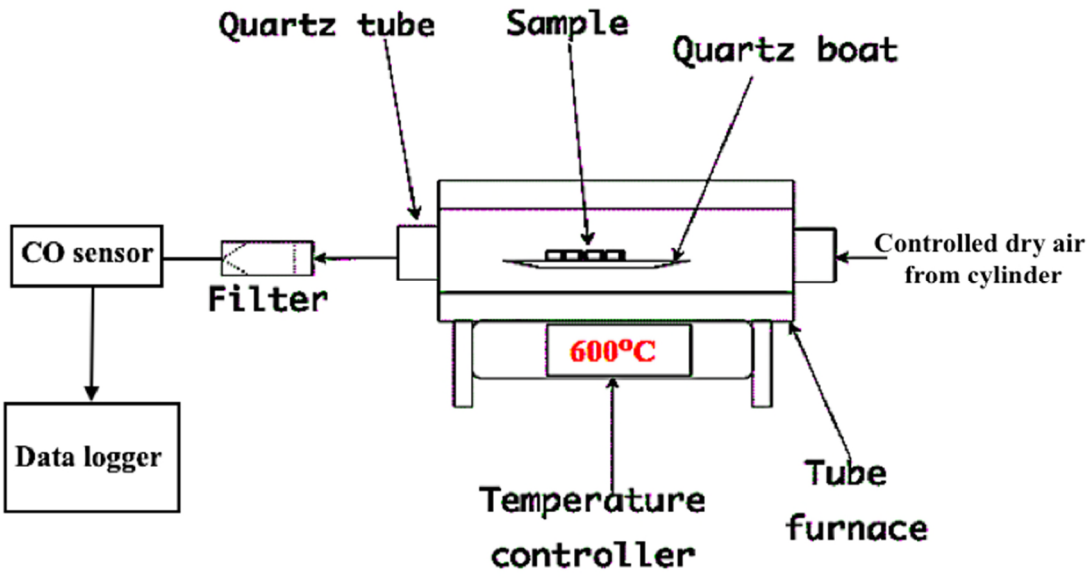

Fig. 1: Schematic of the experimental setup for CO quantification

2.4 Percentage residual CO

The residual amount of carbon monoxide were computed from equation (1) below;

$$CO_{rT}\ (\%) = 100 - \left(\frac{CO_0 - CO_c}{CO_0}\right) * 100 \qquad (1)$$

where, CO_{rT}, CO_0, and CO_c are the residual CO at any temperature T, carbon monoxide from untreated charcoal and carbon monoxide from catalyst treated charcoal.

3 Results and Discussion

This study reports charcoal made safer from CO released by impregnating it with Cu-Mn and Pd-Sn based catalysts. The decomposition profiles of catalysts under air have been reported using thermogravimetric analysis. Phase composition of the as-received, and heat-treated catalysts were analysed using XRD. The composition of the resulting ash after combustion was analysed with XRF. The residual CO recorded as mole CO per mole carbon burnt are presented for untreated charcoal and catalyst-treated-charcoal as a function of temperature.

3.1 Thermogravimetric analysis of catalysts

Fig. 2, shows the TG and DTG thermographs for the Cu-Mn/graphite and Pd-Sn/Alumina catalysts obtained in air (50ml/min) environment at 10°C/min heating rate. The first peak on

the Pd-Sn/alumina profile at 114°C corresponds to the loss of physically bound moisture; the second peak at 272°C corresponds to the loss of chemically bound moisture from $Al(OH)_3$ to form AlOOH. The third peak at 467°C corresponds to the final loss of chemically bound moisture from AlOOH to form Al_2O_3. For the Cu-Mn/graphite TG and DTG profile, the first peak at 114°C corresponds to the loss of physically bound moisture. The second peak at 450 °C corresponds to the conversion of Cu^{2+} to Cu^{+}. The third peak at 500 °C corresponds to the conversion of $Mn^{2.7+}$ to $Mn^{3.2+}$. The forth peak at 550 °C corresponds to the conversion of $Mn^{3.2+}$ to Mn^{3+} and the peak at 660°C could be attributed to the formation of copper metal from its ions. All these phase transformations are supported by X-Ray diffraction analysis performed on the catalysts at as-received samples and after heat treatment at 600°C discussed in the next section.

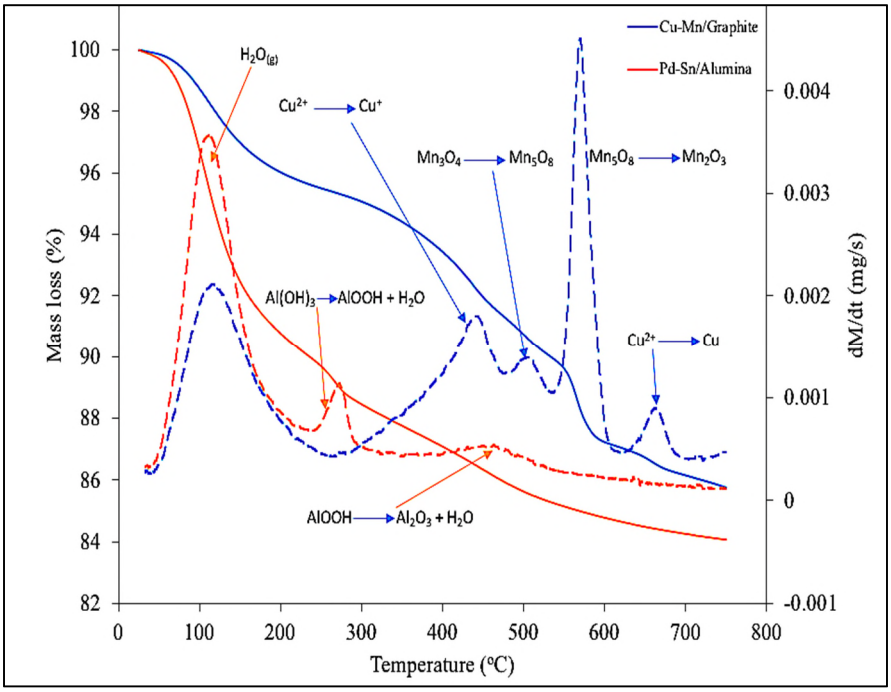

Fig. 2*:* TG and DTG for the Cu-Mn/graphite and Pd-Sn/alumina catalysts obtained in air (50ml/min) environment at 10°C/min heating rate

3.2 X-Ray Diffraction

Fig. 3 (1) and (2) show the diffractograms of Cu-Mn/graphite and Pd-Sn/alumina. The phases MnO_2 (PDF – 30-820), $CuMn_2O_4$ (PDF -74-2422) and Graphite (PDF – 23-64) were identified in the as-received Cu-Mn/graphite catalyst. After heat treatment at 600°C for 3 hours, $Cu_{1.5}Mn_{1.5}O_4$ (PDF – 35-1030), Mn_5O_8 (PDF – 20-718), Mn_2O_3 (PDF – 2-898) and graphite (PDF – 23-64) were identified. The presence of Mn_5O_8, Mn_2O_3 in the heat treated catalyst is consistent with the observations of Augustin *et al*. [25] who monitored phase

transformations of manganese oxides by in-situ calcination of Mn(II) glycolate. In their study, Mn_3O_4 at 18.0° was formed at about 185 °C after the Mn(II) glycolate peaks had disappeared. The decreasing intensity of Mn_3O_4 peaks was accompanied by an increase in the intensity of the Mn_5O_8 at about 350 °C. At 550 °C, the peaks assigned to Mn_5O_8 disappeared after the appearance of the more stable alpha-Mn_2O_3 reflection at 23.2°. Basahel *et al*.[23] also confirmed the presence of $Cu_{1.5}Mn_{1.5}O_4$/CuO after calcination of Cu-Mn catalyst at 550ºC.

For Pd-Sn/Alumina catalyst, the phases AlO(OH) (PDF- 83-2384), $Al_2O_3.3H_2O$ (PDF- 1-287) and Al_2O_3 (PDF – 4-880) were identified in the as-received catalyst. After heat treatment at 600ºC for 3 hours, Al_2O_3 (PDF – 4-880) and PdO (PDF – 882434) were identified. Alumina (Al_2O_3) is mainly manufactured from its hydroxide. If the mother material remains in the final product, it undergoes dehydration forming more crystalline phases with calcination until the most stable phase is formed. The equations (2) and (3), show the dehydration reactions of aluminium hydroxide forming alumina.

$$Al(OH)_3 \rightarrow AlOOH + H_2O \quad (2)$$

$$AlOOH \rightarrow Al_2O_3 + H_2O \quad (3)$$

The masking of the Pd-Sn peaks in the background of the XRD profile before heat treatment could be attributed to their low concentrations in the catalyst mixture relative to the Alumina support. However, after heat treatment at 600ºC, the aluminium hydroxide peaks disappeared, hence, palladium oxide phase could be noticed. This observation is consistent with that of Bi *et al*. [19].

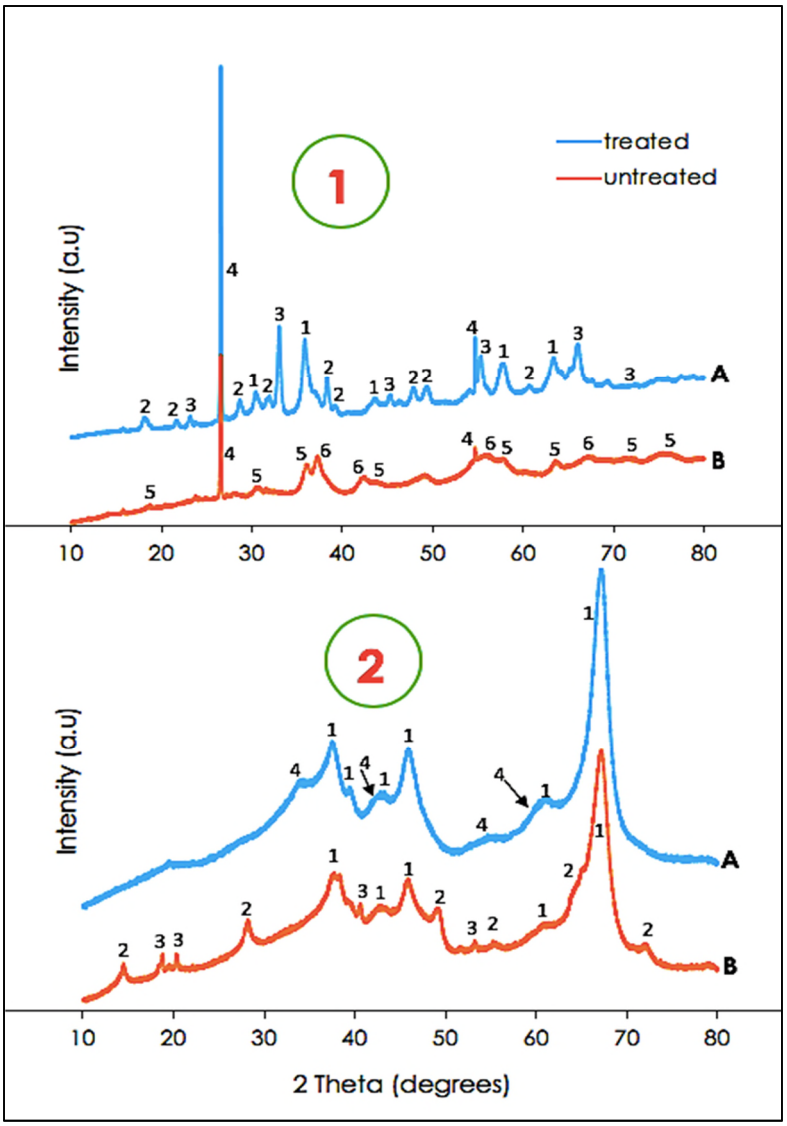

Fig. 3: (1) - XRD profile of Cu-Mn/graphite catalyst: B – before heat treatment and A - after heat treatment at 600°C for 3 hours. The numbers 1, 2, 3, 4, 5, and 6 represent the phases: $Cu_{1.5}Mn_{1.5}O_4$, Mn_5O_8, Mn_2O_3, C(graphite), $CuMn_2O_4$, and MnO_2 respectively. (2) - XRD profile of Pd-Sn/alumina: A – before heat treatment and B - after heat treatment at 600°C for 3 hours. The numbers 1, 2, 3, and 4 represent the phases: Al_2O_3, AlO(OH), $Al_2O_3.3H_2O$ and PdO respectively.

3.3 X-Ray Fluorescence

The concentrations of trace elements in the residual ash were SiO (43.8 wt%), CaO (29.8wt%), P_2O_5 (13.8wt%), K_2O (10.6wt%), FeO 0.9wt%), MgO (1.2wt%), and Al_2O_3 (0.7wt%). The concentrations of trace elements in charcoal could affect the activity of the catalysts arising from trace metal-catalyst reactions/poisoning. Morris *et al*. [26] showed that palladium catalysts activity could be slowed by sulphur and phosphorus. Secondly, build-up of product gases from combustion also deactivates the palladium catalysts. Palladium catalysts could be regenerated with organic polar solvents. Sulphur also poisons copper catalysts during methanol synthesis which involves reaction of CO with hydrogen [26]. However, the impact of these trace elements on catalyst activity was not investigated in this study.

3.4 The activity of Cu-Mn/graphite and Pd-Sn/alumina catalysts for CO oxidation

Catalysts act by adsorption/chemisorption of species onto their surfaces where reactions later take place. Carbon monoxide is adsorbed onto the Pd (111) at the binding sites (Atop, Bridge, FCC, and Hcp). Chen *et al*. [27] observed that lower saturation coverage of CO and lower CO binding energies contributes to the outstanding activity on Pd surfaces. Hsu *et al*. [28] found that the Mn dopant facilitates oxygen vacancy formation, while the Mn adatoms may restrain oxygen vacancy formation. The physisorbed CO, and chemisorbed CO species were also observed on the Mn catalyst. Janki *et al.* [29] found that oxygen atoms on Pd surface increase the binding energy due to lateral repulsion between oxygen atoms and Pd surface. Oxygen interaction with Pd brings about a strong electrostatic repulsion between adsorbates which is responsible for the adsorption energy to decrease with increasing coverage. There is a general decrease in heats of chemisorption on transition metal surfaces with CO and O_2 coverage and could be linked to the metallic radius of the metals [15].

Fig. 4, shows the residual amounts of CO recorded for catalyst treated charcoal. The residual CO from catalyst-treated charcoal were recorded at temperatures 300-600^{o}C and 2L/min dry compressed air flow were. The CO amounts followed a non-linear trend with temperature. Morris *et al*. [26] showed that Pd and Cu based catalysts are denatured at high temperatures through a sintering process. They proposed that use of reaction temperatures lower than 1/3 to ½ of the melting point of the metal catalysts would minimise catalyst sintering. These observations are consistent with those of Ivanov *et al*.[30] and others [19], [23].

On impregnation of the charcoal with 5w% Cu-Mn/graphite catalyst, the residual amounts of CO measured were 16.7% and 42.7% as lowest and highest. With 2w% Cu-Mn/graphite catalyst, the residual amounts of CO were 15.6% and 25.3% as lowest and highest. Increasing the amount of catalyst impregnated onto the charcoal increases the active sites for adsorption of CO and O_2 for better CO oxidation [15]. On the other hand, mixing of the charcoal with Pd-Sn/alumina released less CO than the Cu-Mn/graphite treated charcoal. With the 1w% Pd-Sn/alumina catalyst, only 3.5% and 31.6% were recorded as the lowest and highest residual CO amounts. When the concentrations were reduced to 0.2w%, the residual CO amounts recorded were 26.9% and 44.4% as the lowest and highest respectively. These data together with CO levels from charcoal without catalyst are provided in supplementary data. The enhanced activity with catalyst loading is consistent with observations of Bi *et al*.[19].

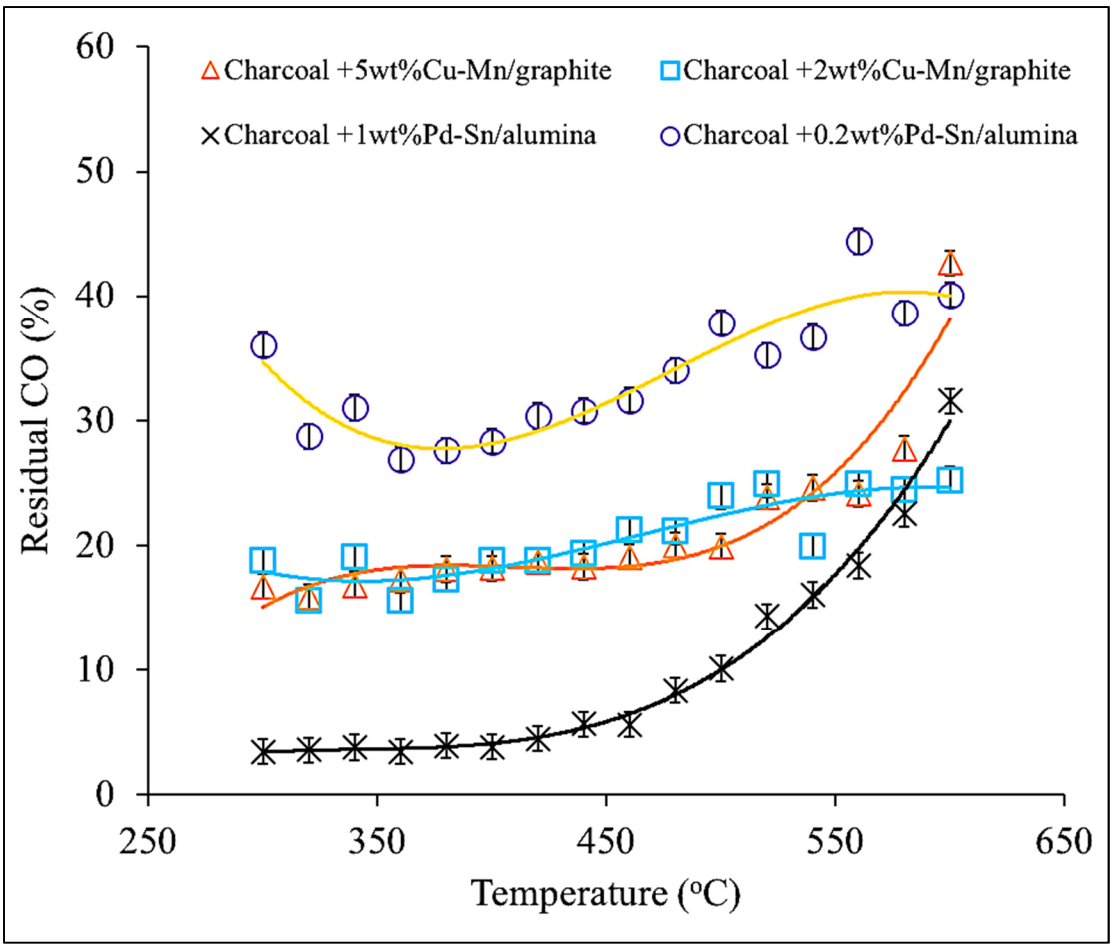

Fig. 4: Residual CO recorded for catalyst treated charcoal

4 Conclusions

In this study, charcoal was for the first time mechanically impregnated with catalysts to minimize carbon monoxide released during combustion. Two commercial catalysts were used: Pd-Sn/alumina and Cu-Mn/graphite. With 1wt% of Pd-Sn/alumina impregnated on charcoal, 3.5% was observed as lowest residual CO. When the concentrations were reduced to 0.2wt% Pd-Sn/alumina, 26.9% was recorded as lowest residual CO. On the other hand, when 5wt% of Cu-Mn/graphite was impregnated, 16.7% was achieved as lowest residual CO. With 2wt% Cu-Mn/graphite, 15.6% was achieved as lowest residual CO. Pd-Sn/alumina was a better catalyst for CO oxidation in this study. In all cases of catalyst testing, the activity decreased with temperature and increased with catalyst loading. The decreased activity of catalysts was due to formation of less active phases. It could also be due to trace elements in the ash formed as charcoal burnt. However, the effect of trace elements was not investigated in this study. This study could be scaled-up for commercial production of catalyst treated

charcoal that is safer for domestic and industrial applications. The method could also be used for production of catalyst treated sawdust briquettes, wood boiler chips and other solid materials to minimise the amounts of CO released from combustion reactions.

Acknowledgments

The authors thank the Hazel Woodhams Memorial Fund, Gas Safety Trust, Boat Safety Scheme and Katie Haines for sponsoring this work. Gratitude to Charlene Greenwood, Peter Wilkinson, Nicola Darcy for assisting at different stages of the experimental work.

Competing interests

The authors declare no competing interests.

Data availability statement

All the data associated with this work is available in this manuscript.

References

[1] H.L. Huang, W.M.G. Lee, F.S. Wu, Emissions of air pollutants from indoor charcoal barbecue, J. Hazard. Mater. 302 (2016) 198–207. doi:10.1016/j.jhazmat.2015.09.048.

[2] D. Bosch, Unintentional domestic non-fire related carbon monoxide poisoning: Data from media reports, UK/Republic of Ireland 1986-2011: Fisher DS, Bowskill S, Saliba L, Flanagan RJ. Clin Toxicol (Phila) 2013;51:409-16., J. Emerg. Med. 45 (2013) 312. doi:10.1016/j.jemermed.2013.06.014.

[3] I. Dianat, J. Nazari, Characteristics of unintentional carbon monoxide poisoning in Northwest Iran--Tabriz., Int. J. Inj. Contr. Saf. Promot. 18 (2011) 313–20. doi:10.1080/17457300.2011.589006.

[4] J. Nazari, I. Dianat, A. Stedmon, Unintentional carbon monoxide poisoning in northwest iran: A 5-year study, J. Forensic Leg. Med. 17 (2010) 388–391. doi:10.1016/j.jflm.2010.08.003.

[5] L. Bennetto, L. Powter, N.J. Scolding, Accidental carbon monoxide poisoning presenting without a history of exposure: a case report., J. Med. Case Rep. 2 (2008) 118. doi:10.1186/1752-1947-2-118.

[6] Y.Y. Chen, O. Bennewith, K. Hawton, S. Simkin, J. Cooper, N. Kapur, D. Gunnell, Suicide by burning barbecue charcoal in England, J. Public Heal. (United Kingdom). 35 (2013) 223–227. doi:10.1093/pubmed/fds095.

[7] P.R. Nielsen, A. Gheorghe, N. Lynnerup, Forensic aspects of carbon monoxide poisoning by charcoal burning in Denmark, 2008-2012: An autopsy based study, Forensic Sci. Med. Pathol. 10 (2014) 390–394. doi:10.1007/s12024-014-9574-3.

[8] A.C.W. Lee, Y. Ou, S.Y. Lam, K.T. So, C.W. Kam, Non-accidental carbon monoxide poisoning from burning charcoal in attempted combined homicide-suicide, J. Paediatr. Child Health. 38 (2002) 465–468. doi:10.1046/j.1440-1754.2002.00019.x.

[9] E. Yoshioka, S.J.B. Hanley, Y. Kawanishi, Y. Saijo, Epidemic of charcoal burning suicide in Japan, Br. J. Psychiatry. 204 (2014) 274–282. doi:10.1192/bjp.bp.113.135392.

[10] J.J. Jetter, P. Kariher, Solid-fuel household cook stoves: Characterization of performance and emissions, Biomass and Bioenergy. 33 (2009) 294–305. doi:10.1016/j.biombioe.2008.05.014.

[11] K.R. Smith, M. a K. Khalil, R.A. Rasmussen, S.A. Thorneloe, F. Manegdeg, M. Apte, Greenhouse Gases from Biomass and Fossil-Fuel Stoves in Developing-Countries - a Manila Pilot-Study, Chemosphere. 26 (1993) 479–505. doi:10.1016/0045-6535(93)90440-G.

[12] Q. Li, J. Jiang, J. Qi, J. Deng, D. Yang, J. Wu, L. Duan, J. Hao, Improving the Energy Efficiency of Stoves to Reduce Pollutant Emissions from Household Solid Fuel Combustion in China, Environ. Sci. Technol. Lett. 3 (2016) 369–374. doi:10.1021/acs.estlett.6b00324.

[13] M. Ezzati, B.M. Mbinda, D.M. Kammen, Comparison of emissions and residential exposure from traditional and improved cookstoves in Kenya, Environ. Sci. Technol. 34 (2000) 578–583. doi:10.1021/es9905795.

[14] M.A. Johnson, R.A. Chiang, Quantitative guidance for stove usage and performance to achieve health and environmental targets, Environ. Health Perspect. 123 (2015) 820–826. doi:10.1289/ehp.1408681.

[15] S. Royer, D. Duprez, Catalytic Oxidation of Carbon Monoxide over Transition Metal Oxides, ChemCatChem. 3 (2011) 24–65. doi:10.1002/cctc.201000378.

[16] S. Fuchs, T. Hahn, H.G. Lintz, Oxidation of carbon monoxide by oxygen over platinum, palladium and rhodium catalysts from 10^-10 to 1 bar, Chem. Eng. Process. 33 (1994) 363–369. doi:10.1016/0255-2701(94)02007-8.

[17] Y. Li, Y. Yu, J.G. Wang, J. Song, Q. Li, M. Dong, C.J. Liu, CO oxidation over graphene supported palladium catalyst, Appl. Catal. B Environ. 125 (2012) 189–196. doi:10.1016/j.apcatb.2012.05.023.

[18] M.D. Esrafili, P. Nematollahi, R. Nurazar, Pd-embedded graphene: An efficient and highly active catalyst for oxidation of CO, Superlattices Microstruct. 92 (2016) 60–67. doi:10.1016/j.spmi.2016.02.006.

[19] Y. Bi, G. Lu, Catalytic CO oxidation over palladium supported NaZSM-5 catalysts, Appl. Catal. B Environ. 41 (2003) 279–286. doi:10.1016/S0926-3373(02)00166-2.

[20] F. Wang, Y. Xu, K. Zhao, D. He, Preparation of Palladium Supported on Ferric Oxide Nano-catalysts for Carbon Monoxide Oxidation in Low Temperature, Nano-Micro Lett. 6 (2014) 233–241. doi:10.1007/BF03353787.

[21] S.A. Kondrat, T.E. Davies, Z. Zu, P. Boldrin, J.K. Bartley, A.F. Carley, S.H. Taylor, M.J. Rosseinsky, G.J. Hutchings, The effect of heat treatment on phase formation of copper manganese oxide: Influence on catalytic activity for ambient temperature carbon monoxide oxidation, J. Catal. 281 (2011) 279–289. doi:10.1016/j.jcat.2011.05.012.

[22] E.C. Njagi, C.-H. Chen, H. Genuino, H. Galindo, H. Huang, S.L. Suib, Total oxidation of CO at ambient temperature using copper manganese oxide catalysts prepared by a redox method, Appl. Catal. B Environ. 99 (2010) 103–110. doi:10.1016/j.apcatb.2010.06.006.

[23] S.N. Basahel, E.H. El Mossalamy, M. Mokhtar, Preparation and physicochemical characterisation of thermally stable nano-sized hopcalite catalysts, Int. J. Nanomanuf. 4 (2009) 159. doi:10.1504/IJNM.2009.028122.

[24] T.J. Clarke, T.E. Davies, S.A. Kondrat, S.H. Taylor, Mechanochemical synthesis of copper manganese oxide for the ambient temperature oxidation of carbon monoxide, Appl. Catal. B Environ. 165 (2015) 222–231. doi:10.1016/j.apcatb.2014.09.070.

[25] M. Augustin, D. Fenske, I. Bardenhagen, A. Westphal, M. Knipper, T. Plaggenborg, J. Kolny-Olesiak, J. Parisi, Manganese oxide phases and morphologies: A study on calcination temperature and atmospheric dependence, Beilstein J. Nanotechnol. 6 (2015) 47–59. doi:10.3762/bjnano.6.6.

[26] M. Argyle, C. Bartholomew, Heterogeneous Catalyst Deactivation and Regeneration: A Review, Catalysts. 5 (2015) 145–269. doi:10.3390/catal5010145.

[27] R. Chen, Z. Chen, B. Ma, X. Hao, N. Kapur, J. Hyun, K. Cho, B. Shan, CO adsorption on Pt (111) and Pd (111) surfaces: A first-principles based lattice gas Monte-Carlo study, Comput. Theor. Chem. 987 (2012) 77–83. doi:10.1016/j.comptc.2011.07.015.

[28] L.-C. Hsu, M.-K. Tsai, Y.-H. Lu, H.-T. Chen, Computational Investigation of CO Adsorption and Oxidation on Mn/CeO_2 (111) Surface, J. Phys. Chem. C. 117 (2013)

433–441. doi:10.1021/jp310457g.

[29] J. Shah, S. Kansara, S.K. Gupta, Y. Sonvane, Oxygen adsorption on palladium monolayer as a surface catalyst, Phys. Lett. Sect. A Gen. At. Solid State Phys. 381 (2017) 3084–3088. doi:10.1016/j.physleta.2017.07.024.

[30] K.I. Ivanov, E.N. Kolentsova, D.Y. Dimitrov, Alumina Supported Copper-Manganese Catalysts for Combustion of Exhaust Gases : Effect of Preparation Method, Int. J. Chem. Mol. Nucl. Mater. Metall. Eng. 9 (2015) 298–307.

Supplementary Data

Table 1: Amounts of CO (mol/mol) from charcoal without catalyst and corresponding CO (mol/mol) from catalyst treated charcoal and computed residual CO (%)

	Charcoal without catalyst		Charcoal + 5wt% Cu-Mn/graphite			Charcoal + 2wt% Cu-Mn/graphite			Charcoal + 1wt% Pd-Sn/alumina			Charcoal + 0.2w% Pd-Sn/alumina		
Temp (°C)	CO/C (mol/mol)	STD	CO/C (mol/mol)	STD	Residual CO (%)	CO/C (mol/mol)	STD	Residual CO (%)	CO/C (mol/mol)	STD	Residual CO (%)	CO/C (mol/mol)	STD	Residual CO (%)
300	0.1523	0.0164	0.0255	0.0015	16.7	0.0287	0.0045	18.8	0.0053	0.0009	3.5	0.0549	0.0048	36.1
320	0.1735	0.0051	0.0295	0.0017	17.0	0.0271	0.0007	15.6	0.0062	0.0001	3.6	0.0498	0.0008	28.7
340	0.1682	0.0259	0.0283	0.0001	16.8	0.0321	0.0057	19.1	0.0064	0.0001	3.8	0.0522	0.0042	31.0
360	0.1902	0.0000	0.0328	0.0005	17.2	0.0297	0.0007	15.6	0.0066	0.0000	3.5	0.0512	0.0004	26.9
380	0.1820	0.0083	0.0330	0.0008	18.1	0.0315	0.0016	17.3	0.0072	0.0008	3.9	0.0502	0.0004	27.6
400	0.1902	0.0029	0.0346	0.0021	18.2	0.0358	0.0006	18.8	0.0073	0.0006	3.8	0.0539	0.0010	28.3
420	0.1904	0.0053	0.0357	0.0028	18.7	0.0359	0.0003	18.9	0.0086	0.0004	4.5	0.0578	0.0017	30.4
440	0.1927	0.0076	0.0353	0.0056	18.3	0.0374	0.0005	19.4	0.0109	0.0004	5.7	0.0593	0.0049	30.8
460	0.1858	0.0059	0.0355	0.0018	19.1	0.0395	0.0004	21.2	0.0105	0.0028	5.6	0.0588	0.0022	31.6
480	0.1775	0.0083	0.0356	0.0008	20.0	0.0375	0.0022	21.1	0.0148	0.0004	8.4	0.0604	0.0016	34.0
500	0.1777	0.0005	0.0355	0.0028	20.0	0.0426	0.0002	24.0	0.0180	0.0015	10.1	0.0672	0.0015	37.8
520	0.1789	0.0049	0.0427	0.0043	23.9	0.0446	0.0002	24.9	0.0256	0.0013	14.3	0.0630	0.0030	35.2
540	0.1897	0.0009	0.0467	0.0024	24.6	0.0379	0.0010	20.0	0.0305	0.0021	16.1	0.0697	0.0018	36.7
560	0.1823	0.0020	0.0440	0.0004	24.2	0.0455	0.0007	24.9	0.0335	0.0002	18.4	0.0809	0.0019	44.4
580	0.1985	0.0012	0.0551	0.0022	27.8	0.0486	0.0021	24.5	0.0447	0.0028	22.5	0.0767	0.0017	38.6
600	0.2118	0.0474	0.0904	0.0006	42.7	0.0535	0.0000	25.3	0.0669	0.0033	31.6	0.0850	0.0025	40.1